

Supplement of *Clim. Past*, 19, 1061–1079, 2023
<https://doi.org/10.5194/cp-19-1061-2023-supplement>
© Author(s) 2023. CC BY 4.0 License.



Supplement of

Deglacial and Holocene sea-ice and climate dynamics in the Bransfield Strait, northern Antarctic Peninsula

Maria-Elena Vorrath et al.

Correspondence to: Juliane Müller (juliane.mueller@awi.de)

The copyright of individual parts of the supplement might differ from the article licence.

Supplements

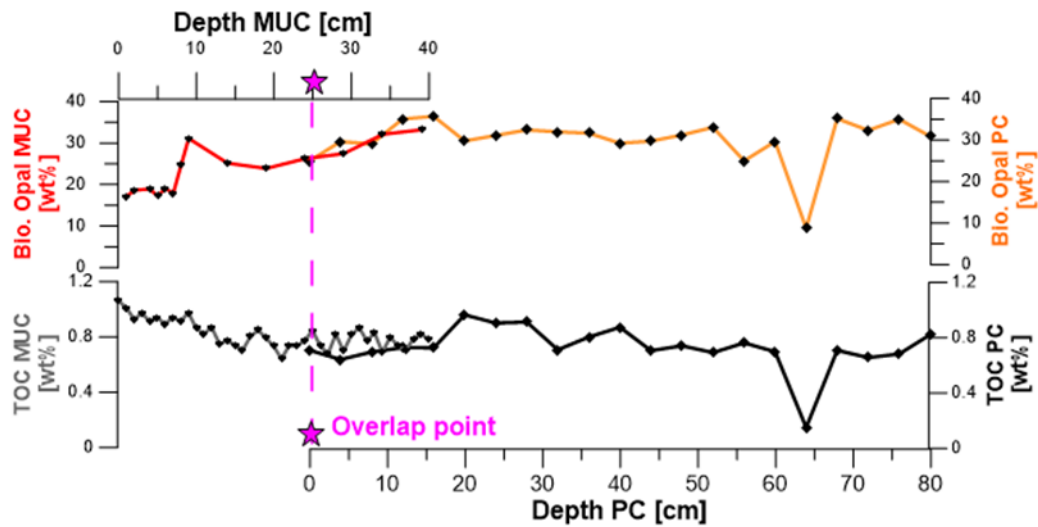
S1: Radiocarbon dating

Table S1: Overview of radiocarbon data including sample name and number, material, conventional age plus error, the modelled age for correction, ventilation age, corrected age and final calibrated ages with error. Due to the lack of planktic foraminifera, we base the age model of core PS97/072-1 on benthic AMS ^{14}C dates obtained from shell fragments and benthic foraminifera tests. This is usually done without problems on shallow shelves (< 400 m) where the benthos lives in a mixed layer - or in areas where nearby paired benthic-planktic AMS ^{14}C ages provide a ^{14}C -ventilation age for bottom waters that can be subtracted in addition to surface reservoir ages in the calibration routine. To account for the relatively deep water depth (ca. 2000 m) at core site PS97/072-1, we added a ventilation age of 1200 years to the surface reservoir age to account for the additional age of deep water masses relative to the surface waters. This is needed as Butzin et al. (2017) we use here only accounts for a reservoir age of the upper water masses between 0 - 300 m. Our estimation of ventilation age is based on paired planktic and benthic foraminifera of 1000 to 15000 years found off Chile (Siani et al., 2013) and the Kerguelen Islands (Gottschalk et al., 2020). Further, earlier comparisons of dated benthic calcareous material with AIOM-derived ^{14}C ages, which had been in turn compared to planktic foraminiferal ages in various locations at the Antarctic Peninsula (Domack et al., 2001; Barcena et al., 2006; Heroy et al., 2008), as well as ^{14}C ages of deep-water corals from nearby Drake Passage, independently dated by U/Th (Burke and Robinson, 2012), indicate radiocarbon ventilation ages between ca. 1100-1400 years as acceptable approach. For the calibration of the (reservoir and ventilation age corrected) ^{14}C dates, we used the IntCal20 curve as this calibration does not automatically subtract “time-varying” marine reservoir ages as the new Marine20 curve. This allowed us to subtract the reservoir and ventilation ages individually based on our assumptions.

Sample depth [cmbsf]	Sample Name	AWI-No.	Material	Conventional ^{14}C age [a BP]	Error conv. ^{14}C age [a]	Modelled age for correction after Butzin et al. (2017) [a]	Ventilation age for correction [a]	Corrected ^{14}C age for calibration [a BP]	Calibrated age [cal. a BP]	Error of calibrated age 1 sigma [a]	Error of calibrated age 2 sigma [a]
190	PS97/072-1_190cm	1428.1.1	shell fragments	5076	118	1076	1200	2800	2920	140	300
212	PS97/072-1_212cm	2744.1.1	shell fragments	5246	82	1107	1200	2939	3090	120	230
312	PS97/072-1_312cm	1429.2.1	shell fragments	6054	118	1083	1200	3771	4170	190	340
340	PS97/072-1_340cm	1430.1.1	shell fragments	6156	52	1089	1200	3867	4300	110	160
451.5	PS97/072-1_451.5cm	1431.1.1	shell fragments	7081	52	1142	1200	4739	5410	80	130
464	PS97/072-1_464cm	1432.2.1	shell fragments	7329	117	1157	1200	4972	5740	150	260
866.5	PS97/072-1_866.5cm	7405.1.1	benthic foraminifer	12865	101	1599	1200	10066	11610	210	330
868.5	PS97/072-1_868.5cm	7406.1.1	benthic foraminifer	12983	100	1571	1200	10212	12040	390	530

S2: Matching piston core PS97/072-1 and short core PS97/072-2

We matched the top of piston core PS97/072-1 with the short core PS97/072-2 from the same sample site using TOC and biogenic opal data (Fig. S1). An age model for the short core was already developed based on ^{210}Pb dating (Vorrath et al., 2020). By overlapping the TOC and biogenic opal records we note that the top of the piston core likely matches the short core at a depth of 25 cm, which corresponds to the calendar year 1902 in the common era. Therefore, we have set the age of the core top of PS97/072-1 to 0.05 ka BP.



32

33 Figure S2: Overlap point of the short sediment core PS97/072-2 (MUC) and piston core PS97/072-1 (PC) based
 34 on total organic carbon and biogenic opal (wt%). Data from the short core from Vorrath et al. (2020).

35

36

37

38 **S3:** Taxonomic list of diatoms identified in the sediments of core PS97/072-1 organized by groups according to
 39 their habitat (Armand et al., 2005; Cárdenas et al., 2019; Crosta et al., 2005; Esper et al., 2010; Esper and Gersonde,
 40 2014a, 2014b; Gersonde and Zielinski, 2000; Romero et al., 2005; Zielinski and Gersonde, 1997).

41

42 **Benthic and epiphytic diatoms:**

43 *Achnanthes brevipes* Agardh

44 *Amphora copulata* (Kützing) Kützing

45 *A. coffaeiformis* (Agardh) Kützing

46 *Cocconeis costata* Gregory

47 *C. dalmanii* Al-Handal, Riaux-Gobin, Romero & Wulff

48 *C. fasciolata* (Ehrenberg) Brown

49 *C. californica* var. *californica* Grunow

50 *C. californica* var. *keguelensis* Heiden

51 *C. melchioroides* Al-Handal, Riaux-Gobin, Romero & Wulff

52 *C. imperatrix* Schmidt

53 *C. schuettii* Van Heurck

54 *Cocconeis* spp.

55 *Entopyla ocellata* (Arnott) Grunow

56 *Fallacia marnieri* (Manguin) Witkowski, Lange-Bertalot & Metzeltin

57 *Gomphonemopsis littoralis* (Hendey) Medlin

58 *Grammatophora angulosa* Ehrenberg

59 *Licmophora gracilis* (Kützing) Peragallo

60 *Melosira adeliae* Manguin

61 *Navicula directa* (Smith) Ralfs

62 *N. glaciei* Van Heurck

63 *N. imperfecta* Cleve

64 *N. perminuta* Grunow

65 *Paralia sulcata* (Ehrenberg) Cleve

66 *Planothidium vicentii* Manguin

67 *Pseudogomphonema kamtschaticum* (Grunow) Medlin

68

69 **Diatoms reflecting seasonal sea-ice (temperature range between -1.8 and 0°C):**

- 70 *Actinochilus* (Ehrenberg) Simonsen
71 *Berkeleya adeliensis* Medlin
72 *B. antarctica* Grunow
73 *B. rutilans* (Trentepohl) Grunow
74 *Corethron pennatum* (Grunow) Ostenfeld
75 *Eucampia antarctica* var. *recta* Mangin
76 *Fragilariopsis curta* (Van Heurck) Hustedt
77 *F. cylindrus* (Grunow) Krieger
78 *F. nana* (Steeemann Nielsen) Paasche
79 *F. obliquecostata* (Van Heurck) Heiden
80 *F. peragallii* (Hasle) Cremer
81 *F. rhombica* (O'Meara) Hustedt
82 *F. ritscheri* Hustedt
83 *F. sublinearis* (Van Heurck) Heiden & Kolbe
84 *F. vanheurckii* (Peragallo) Hustedt
85 *Nitzschia hybrida* Grunow
86 *N. stellata* Manguin
87 *N. taeniiformis* Simonsen
88 *Odontella weissflogii* (Janisch) Grunow *Porosira glacialis* (Grunow) Jørgensen
89 *Porosira pseudodenticulata* (Hustedt) Jousé
90 *Stellarima microtrias* (Ehrenberg) Hasle & Sims
91 *Synedropsis laevis* (Heiden) Hasle, Medlin & Syvertsen
92 *S. recta* Hasle, Syvertsen & Medlin
93 *Synedropsis* sp.
94 *Thalassiosira antarctica* (T1) Comber

95
96 **Diatoms associated with cold open ocean conditions (temperature range between 1 and 4°C):**

- 97 *Asteromphalus hookeri* Ehrenberg
98 *A. hyalinus* Karsten
99 *Eucampia antarctica* var. *antarctica* Mangin
100 *Fragilariopsis pseudonana* (Hasle) Hasle
101 *F. separanda* Hustedt
102 *Proboscia alata* (Brightwell) Sundström
103 *P. inermis* (Castracane) Hordan & Ligowski
104 *Proboscia* sp.
105 *Pseudo-nitzschia turgiduloides* Hasle
106 *Rhizosolenia antennata* f. *antennata* Sundström
107 *R. antennata* f. *semispina* Sundström
108 *R. polydactyla* f. *polydactyla* Castracane
109 *R. simplex* Karsten
110 *Shionodiscus frenguelliopsis* (Fryxell & Johansen) Alverson, Kang & Theriot
111 *S. gracilis* var. *expectus* (VanLandingham) Alverson, Kang & Theriot
112 *S. gracilis* var. *gracilis* (Karsten) Alverson, Kang & Theriot
113 *Thalassiosira antarctica* (T2) Comber
114 *T. gravida* Cleve
115 *T. lentiginosa* (Janisch) Fryxell
116 *T. maculata* Fryxell & Johansen
117 *T. oliverana* Priddle & Fryxell
118 *T. ritscheri* (Hustedt) Hasle
119 *T. scotia* Fryxell & Hoban
120 *T. tumida* (Janisch) Hasle
121 *Thalassiothrix antarctica* Schimper ex Karsten
122 *Trichotoxon reinboldii* (Van Heurck) Reid & Round

123
124
125
126
127
128
129
130
131
132
133
134
135
136
137
138
139
140
141
142
143
144
145
146
147
148
149
150
151
152
153
154
155
156
157
158
159
160
161
162
163
164
165
166
167
168
169
170
171
172
173
174
175
176

Diatoms associated with warmer open ocean conditions (temperature range between 4 and 14°C):

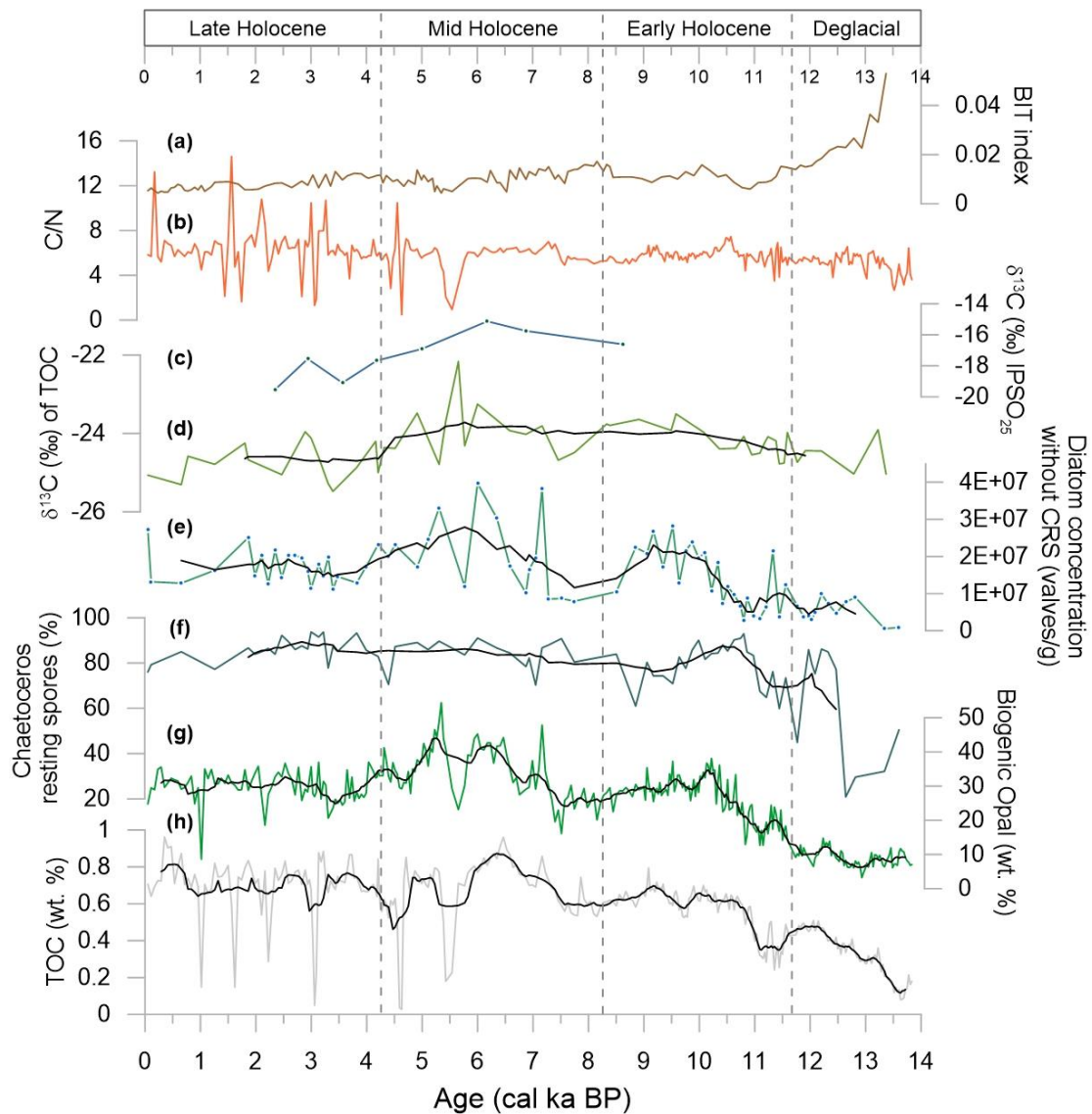
- Azpeitia tabularis* (Grunow) Fryxell & Sims
Coscinodiscus oculus-iridis (Ehrenberg) Ehrenberg
Fragilariopsis kerguelensis (O'Meara) Hustedt
Nitzschia bicapitata Cleve
Shionodiscus oestrupii (Ostenfeld) Alverson, Kang & Theriot
Stephanopyxis turris Greville & Arnott

Reworked species:

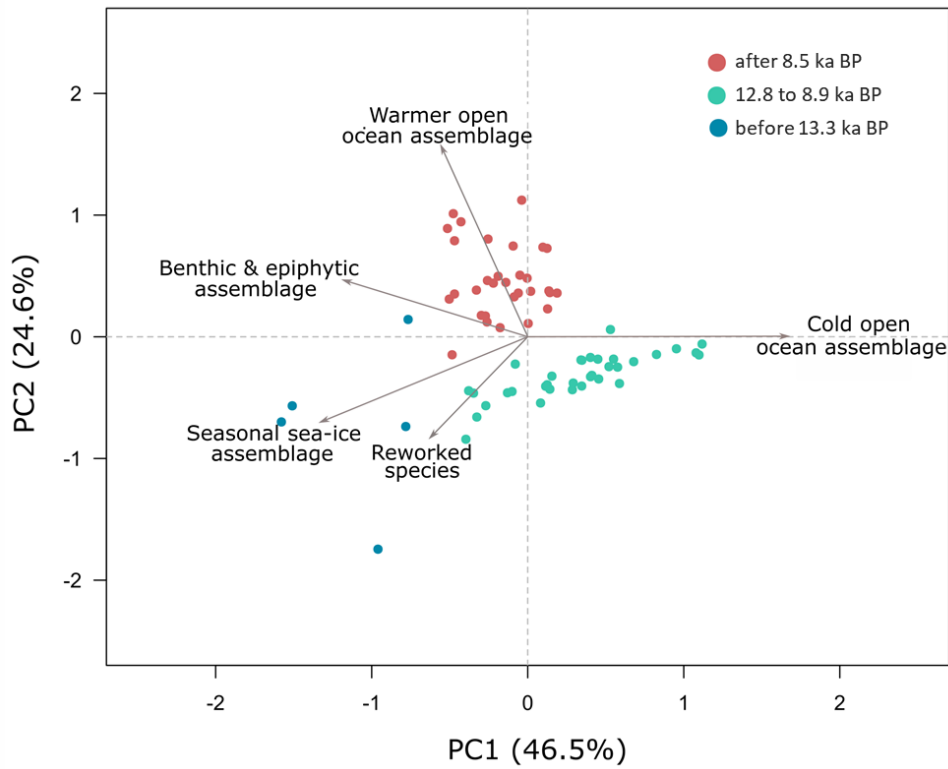
- Actinocyclus ingens* Rattray
Cladogramma sp. Lohmann
Denticulopsis spp. (Simonsen)
Rouxia constricta Zielinski & Gersonde
R. leventerae Bohaty, Scherer & Harwood

177 **S4: Terrigenous input, stable isotopes of TOC and IPSO₂₅, and total diatom and CRS content**

178 The BIT indices below 0.05 and the mean molar C/N ratio below 8.5 indicate a marine origin of the organic matter
 179 and that the input of terrigenous organic matter did not affect the composition of GDGTs. Maximum BIT values
 180 of up to 0.05 between 13.5 ka and 12.0 ka BP may evidence an additional input of soil-derived GDGTs in response
 181 to glacier activity. However, these values are distinctly lower than the 0.3 threshold signaling enhanced input of
 182 terrigenous organic matter and since also the C/N values do not point to higher input of terrestrial material during
 183 this time interval, we conclude that the GDGT paleothermometry was not affected by soil-derived GDGTs.
 184 Organic carbon stable isotope ratios ($\delta^{13}\text{C}$) range between -22.2 and -25.5‰, while the stable carbon isotope
 185 composition of IPSO₂₅ varies between -15.1‰ and -19.5‰ supporting its origin from sea ice algae (Massé et al.,
 186 2011; Sinninghe Damsté et al., 2007). Also shown are total diatom concentrations (without *Chaetoceros* resting
 187 spores) and percentage of *Chaetoceros* resting spores in comparison to biogenic opal and TOC content.
 188



189
 190
 191 Figure S4: Comparison of biomarkers and selected diatom count data with stable carbon isotope composition of
 192 organic material a) BIT index, b) C/N values, c) $\delta^{13}\text{C}$ of IPSO₂₅, d) $\delta^{13}\text{C}$ of TOC, e) total diatom concentration, f)
 193 *Chaetoceros* resting spores, g) biogenic opal content, and h) TOC content of PS97/072-1.
 194



196
 197 Figure S5: The Spearman principal component analysis (PCA) biplot shows the relationship between the five
 198 diatom assemblages indicative for a warmer open and colder open ocean, seasonal sea-ice, benthic/epiphytic, and
 199 reworked diatoms in core PS97/072-1. PC1 represents 46.5% and PC2 24.6% of the variance. Before 13.3 ka BP
 200 seasonal sea-ice diatoms are common, between 12.8 ka and 8.9 ka BP assemblages of a colder open ocean are
 201 dominant whereas a warmer open ocean is indicated by diatom assemblages from 8.5 ka BP until today.
 202
 203
 204

205 **S6: Details on principal component analysis**

206 Diatom assemblages, and ages scores of Principal Component Analysis (PCA), eigenvalues and percentage of
 207 variance explained from figure S5. The diatom assemblages can be found in the online resource
 208 (<https://doi.pangaea.de/10.1594/PANGAEA.952279>).
 209

Importance of components						
		PC1	PC2	PC3	PC4	PC5
Eigenvalue		2.326	1.236	0.928	0.491	0.018
Proportion explained		0.465	0.247	0.186	0.098	0.004
Cumulative proportion of variance		0.465	0.713	0.898	0.996	1
Species scores						
Assemblages		PC1	PC2	PC3	PC4	PC5
Benthic and epiphytic		-1.375	0.600	-0.558	1.034	0.017
Seasonal sea ice		-1.560	-0.722	0.799	-0.114	0.164
Open ocean cold		1.837	0.061	-0.338	0.326	0.184
Open ocean warm		-0.592	1.668	-0.255	-0.655	0.073
Reworked species		-0.633	-0.908	-1.497	-0.408	0.027
Scores (weight sums of assemblages scores)						
Depth in core (cm)	Age [ka cal BP]	PC1	PC2	PC3	PC4	PC5
4	0.111	-0.178	0.455	-0.361	1.108	0.262
40	0.657	-0.184	0.499	-0.541	1.664	0.061
80	1.265	-0.257	0.171	0.138	0.001	-0.175
120	1.872	0.022	0.096	0.176	-0.396	-0.055
128	1.994	0.082	0.354	-0.156	0.075	-1.231
136	2.115	0.135	0.732	-0.345	-0.054	0.264
144	2.237	-0.339	0.374	0.035	0.042	-0.377
152	2.358	-0.451	0.368	0.004	0.410	0.624
160	2.480	-0.020	0.351	0.000	-0.236	0.228
168	2.601	-0.010	0.498	-0.062	-0.343	0.285
176	2.723	0.056	0.370	-0.141	0.123	0.229
184	2.844	-0.430	0.792	-0.327	0.580	-0.375
192	2.950	0.210	0.357	-0.219	0.191	0.117
200	3.009	-0.493	-0.166	0.479	-0.163	-0.628
216	3.139	-0.477	0.310	0.012	0.528	0.294
224	3.223	-0.049	0.317	-0.062	-0.343	0.450
232	3.307	-0.206	0.804	-0.362	0.351	-0.164
240	3.392	-0.078	0.464	-0.359	0.943	0.551
248	3.476	-0.224	0.128	-0.108	0.562	0.248
280	3.814	-0.458	0.890	-0.212	0.035	0.425
360	4.511	-0.268	0.610	0.015	-0.474	0.312
400	4.935	-0.303	0.559	-0.059	-0.037	0.296
440	5.359	0.268	0.272	0.123	-0.984	-0.143
480	5.973	-0.391	0.904	0.282	-1.910	0.435

Scores (weight sums of assemblages scores)						
Depth in core (cm)	Age [ka cal BP]	PC1	PC2	PC3	PC4	PC5
520	6.557	0.151	0.214	0.085	-0.503	0.270
540	6.849	0.042	0.472	-0.062	-0.382	0.081
568	7.258	0.000	1.095	-0.200	-1.254	-0.795
584	7.491	-0.418	0.998	-0.137	-0.558	0.197
600	7.725	-0.050	0.745	-0.236	-0.252	-0.578
652	8.484	-0.133	0.082	-0.047	0.671	-0.407
676	8.834	0.627	-0.212	-0.067	0.145	-1.488
690	9.039	0.364	-0.201	0.111	-0.054	-0.437
710	9.331	0.565	-0.249	0.017	0.134	0.298
730	9.622	0.311	-0.443	0.269	0.041	0.383
738	9.739	0.067	-0.402	0.245	0.325	-1.010
746	9.856	0.159	-0.437	0.290	0.179	0.258
754	9.973	-0.095	-0.460	0.424	0.110	-0.121
762	10.090	0.172	-0.334	0.281	-0.047	0.156
770	10.206	0.580	-0.256	0.079	-0.129	-0.106
778	10.323	-0.330	-0.469	0.499	0.281	0.851
784	10.411	-0.314	-0.575	0.505	-0.104	-0.271
790	10.498	-0.396	-0.685	0.835	-0.453	-0.440
798	10.615	-0.394	-0.863	0.995	-0.597	0.322
806	10.732	0.100	-0.554	0.467	-0.113	0.335
810	10.790	0.486	-0.349	0.116	0.107	0.175
814	10.849	0.316	-0.380	0.173	0.249	0.447
822	10.965	0.056	-0.420	0.365	-0.022	-0.418
830	11.082	0.418	-0.321	0.151	0.020	0.129
838	11.199	-0.180	-0.243	0.415	-0.251	-0.736
846	11.316	0.553	0.055	-0.127	-0.004	0.157
854	11.432	0.376	-0.194	0.038	0.060	-2.221
862	11.549	-0.179	-0.445	0.512	-0.079	0.486
870	11.814	1.151	-0.057	-0.379	0.236	0.116
878	11.931	0.857	-0.139	-0.364	0.422	0.279
886	12.048	0.986	-0.098	-0.344	0.056	0.281
890	12.107	1.110	-0.131	-0.289	0.141	0.184
894	12.166	1.135	-0.142	-0.303	0.174	0.138
902	12.283	0.418	-0.178	0.032	-0.171	0.373
910	12.400	0.591	-0.367	0.095	0.066	0.223
920	12.547	0.427	-0.334	0.142	0.080	0.289
932	12.723	0.367	-0.414	0.275	-0.118	0.569
944	12.899	-0.355	-0.453	0.174	-0.368	0.134
980	13.427	-0.865	-1.699	-3.482	-0.984	-0.079
1000	13.721	-1.601	-0.704	0.383	0.483	0.031

References

- Armand, L. K., Crosta, X., Romero, O. and Pichon, J.-J.: The biogeography of major diatom taxa in Southern Ocean sediments: 1. Sea ice related species, *Palaeogeography, Palaeoclimatology, Palaeoecology*, 223(1–2), 93–126, doi:10.1016/J.PALAEO.2005.02.015, 2005.
- Barcena, M.Á., Canals, M., Fabrès, J., Flores, J.A., Isla, E., Palanques, A. and Sierro, F.J.: Holocene neoglacial events in the Bransfield Strait (Antarctica). Palaeoenvironmental and paleoclimatic significance. *Scientia Marina* 70, 607–619, 2006.
- Burke, A. and L. F. Robinson: The Southern Ocean's Role in Carbon Exchange During the Last Deglaciation. *Science* 335(6068): 557–561, 2012.
- Cárdenas, P., Lange, C. B., Vernet, M., Esper, O., Srain, B., Vorrath, M.-E., Ehrhardt, S., Müller, J., Kuhn, G., Arz, H. W., Lembke-Jene, L., Lamy, F.: Biogeochemical proxies and diatoms in surface sediments across the Drake Passage reflect oceanic domains and frontal systems in the region, *Progress in Oceanography*, 174, 72–88, doi:10.1016/j.pocean.2018.10.004, 2019.
- Crosta, X., Romero, O., Armand, L. K. and Pichon, J.-J.: The biogeography of major diatom taxa in Southern Ocean sediments: 2. Open ocean related species, *Palaeogeography, Palaeoclimatology, Palaeoecology*, 223(1–2), 66–92, doi:10.1016/j.palaeo.2005.03.028, 2005.
- Domack, E., Leventer, A., Dunbar, R., Taylor, F., Brachfeld, S., Sjunneskogs, C. and ODP Leg 178 Scientific Party: Chronology of the Palmer Deep site, Antarctic Peninsula: a Holocene palaeoenvironmental reference for the circum-Antarctic. *The Holocene*, 11(1), 1–9, doi:10.1191/095968301673881493, 2001.
- Esper, O. and Gersonde, R.: New tools for the reconstruction of Pleistocene Antarctic sea ice, *Palaeogeography, Palaeoclimatology, Palaeoecology*, 399, 260–283, doi:10.1016/J.PALAEO.2014.01.019, 2014a.
- Esper, O. and Gersonde, R.: Quaternary surface water temperature estimations: New diatom transfer functions for the Southern Ocean, *Palaeogeography, Palaeoclimatology, Palaeoecology*, 414, 1–19, doi:10.1016/J.PALAEO.2014.08.008, 2014b.
- Esper, O., Gersonde, R. and Kadagies, N.: Diatom distribution in southeastern Pacific surface sediments and their relationship to modern environmental variables, *Palaeogeography, Palaeoclimatology, Palaeoecology*, 287(1–4), 1–27, doi:10.1016/J.PALAEO.2009.12.006, 2010.
- Gersonde, R. and Zielinski, U.: The reconstruction of late Quaternary Antarctic sea-ice distribution — the use of diatoms as a proxy for sea-ice, 162, 263–286, doi:10.1016/S0031-0182(00)00131-0, 2000.
- Heroy, D. C., Sjunneskog, C. and Anderson, J. B.: Holocene climate change in the Bransfield Basin, Antarctic Peninsula: evidence from sediment and diatom analysis, *Antarctic Science*, 20(01), 69–87, doi:10.1017/S0954102007000788, 2008.
- Massé, G., Belt, S. T., Crosta, X., Schmidt, S., Snape, I., Thomas, D. N. and Rowland, S. J.: Highly branched isoprenoids as proxies for variable sea ice conditions in the Southern Ocean, *Antarctic Science*, 23(05), 487–498, doi:10.1017/S0954102011000381, 2011.
- Romero, O. E., Armand, L. K., Crosta, X. and Pichon, J.-J.: The biogeography of major diatom taxa in Southern Ocean surface sediments: 3. Tropical/Subtropical species, *Palaeogeography, Palaeoclimatology, Palaeoecology*, 223(1–2), 49–65, doi:10.1016/j.palaeo.2005.03.027, 2005.
- Sinninghe Damsté, J. S., Rijpstra, W. I. C., Coolen, M. J. L., Schouten, S. and Volkman, J. K.: Rapid sulfurisation of highly branched isoprenoid (HBI) alkenes in sulfidic Holocene sediments from Ellis Fjord, Antarctica, *Organic Geochemistry*, 38(1), 128–139, doi:10.1016/j.orggeochem.2006.08.003, 2007.
- Vorrath, M.-E., Müller, J., Rebolledo, L., Cárdenas, P., Shi, X., Esper, O., Opel, T., Geibert, W., Muñoz, P., Haas, C., Kuhn, G., Lange, C. B., Lohmann, G. and Mollenhauer, G.: Sea ice dynamics in the Bransfield Strait, Antarctic Peninsula, during the past 240 years: a multi-proxy intercomparison study, *Climate of the Past*, 16(6), 2459–2483, doi:10.5194/cp-16-2459-2020, 2020.
- Zielinski, U. and Gersonde, R.: Diatom distribution in Southern Ocean surface sediments (Atlantic sector): Implications for paleoenvironmental reconstructions, *Palaeogeography, Palaeoclimatology, Palaeoecology*, 129(3–4), 213–250, doi:10.1016/S0031-0182(96)00130-7, 1997.

